



InSAR observations of the 2009 Racha earthquake, Georgia

Elena Nikolaeva^{1,a} and Thomas R. Walter¹

¹Department 2, Physics of the Earth, Helmholtz Center Potsdam, GFZ German Research Center of Geosciences, Potsdam, Germany

^anow at: Ilia State University, Tbilisi, Georgia

Correspondence to: Elena Nikolaeva (elenanikolaeva@hotmail.com)

Received: 15 May 2015 – Published in Nat. Hazards Earth Syst. Sci. Discuss.: 11 August 2015

Accepted: 24 July 2016 – Published: 23 September 2016

Abstract. Central Georgia is an area strongly affected by earthquake and landslide hazards. On 29 April 1991 a major earthquake ($M_w = 7.0$) struck the Racha region in Georgia, followed by aftershocks and significant afterslip. The same region was hit by another major event ($M_w = 6.0$) on 7 September 2009. The aim of the study reported here was to utilize interferometric synthetic aperture radar (InSAR) data to improve knowledge about the spatial pattern of deformation due to the 2009 earthquake. There were no actual earthquake observations by InSAR in Georgia.

We considered all available SAR data images from different space agencies. However, due to the long wavelength and the frequent acquisitions, only the multi-temporal ALOS L-band SAR data allowed us to produce interferograms spanning the 2009 earthquake. We detected a local uplift around 10 cm (along the line-of-sight propagation) in the interferogram near the earthquake's epicenter, whereas evidence of surface ruptures could not be found in the field along the active thrust fault. We simulated a deformation signal which could be created by the 2009 Racha earthquake on the basis of local seismic records and by using an elastic dislocation model. We compared our modeled fault surface of the September 2009 with the April 1991 Racha earthquake fault surfaces and identify the same fault or a sub-parallel fault of the same system as the origin. The patch that was active in 2009 is just adjacent to the 1991 patch, indicating a possible mainly westward propagation direction, with important implications for future earthquake hazards.

1 Introduction

Large tectonic earthquakes often occur in spatial and temporal proximity. In some cases, these earthquakes successively rupture the same fault with a well-defined propagation direction (Lin and Stein 2004; Burgmann et al., 2000). As seen in the North Anatolian Fault (Pondard et al., 2007; Stein et al., 1997) or in the San Andreas Fault (Lin and Stein, 2004), these propagation directions allow for assessment of seismic hazard potential.

One geologically active environment, with numerous damaging earthquakes and landslide hazards occurring during the 20th century, lies in Georgia, specifically the Racha region. It was hypothesized that the Racha ridge region (the Greater Caucasus mountains) is a consequence of repeated earthquakes (Triep et al., 1995). On 29 April 1991, a major earthquake ($M_w = 7.0$) occurred along a blind thrust fault, causing severe damage to infrastructure and triggering other hazards, such as landslides and rockfalls (Arefiev et al., 2006; Jibson et al., 1994). On 7 September 2009, a smaller earthquake ($M_w = 6.0$) occurred in the same region. No clear rupture was observed except small cracks on the road and local small rock and landslide events. For instance, a landslide in the Sachkhere region showed a small, but relevant acceleration that might be associated with this earthquake (Nikolaeva et al., 2014).

Interferometric synthetic aperture radar (InSAR) has been widely used to measure tectonic deformations since the first publication comprehensively applied this method for the Landers earthquake in California (Massonnet et al., 1993). However, the focus has been on the earthquakes with magnitudes much greater than 6, which produce larger deformations (Wang et al., 2004; Funning, 2005; Reilinger et al.,

2000). In this case, the InSAR observations often show clear deformation signals. The cases of small earthquakes are less studied because surface displacements are likely to be insignificant, and there are uncertainties from satellite orbits and/or intervening atmospheric conditions (Bell et al., 2012). However, several papers show that the InSAR can detect surface deformations in the case of shallow events with magnitudes smaller than 4.8 (Dawson and Tregoning, 2007; Bell et al., 2012).

In this study we used data from the ALOS L-band radar satellite to detect the co-seismic surface deformation associated with the earthquake of the moment magnitude $M_w = 6.0$ on 7 September 2009 in the Racha region. Specifically, the aims of this paper are to investigate the ability of InSAR to provide the spatial pattern of deformation due to the 2009 Racha earthquake, to compare observations of geodetic data with a model based on local information about the earthquake and to investigate a link between the 1991 and 2009 earthquakes.

2 Study area

Located at the junction between the Arabian and Eurasian plates, the Caucasus is one of the most seismically active regions in the Alpine–Himalayan collision belt. Georgia, as part of the Caucasus, is located in the central faulted segment (Fig. 1) and has historically experienced earthquakes (the Catalogue of the Caucasus Earthquakes since 550 BC till AD 2000, <http://zeus.wdcb.ru/wdcb/sep/caucasus/welcomen.html>) as well as strong earthquakes in recent times.

The study area belongs to a fold and thrust mountain belt of the Greater Caucasus (Adamia et al., 2010) with shallow northward-dipping faults (Tan and Taymaz, 2006). Consequently, the tectonics are represented mainly by vertical movements (Lilienberg, 1980) as evidenced by the topography (Philip et al., 1989). The geological structure resulting from the tectonic movements represents the thrust-nappe system of the Greater Caucasus (Triep et al., 1995). The nappe system is formed by Cretaceous to Quaternary sediments and locally masks fault traces (Philip et al., 1989).

The analysis of the historical and instrumental seismological record shows that this region is of moderate seismicity (Balassanian et al., 1999). The possibility of extending the catalog of strong events is important for the seismic study of the region (van Westen et al., 2012). Global Positioning System (GPS) measurements have shown that the Caucasus block moves at 13 mm per year in an east–south direction relative to Eurasia and also has a rotational displacement component with respect to Eurasia (Reilinger et al., 2006).

In addition to the seismic activity, the complicated lithological–tectonic composition of the region and strong topographic relief underlines the relevance of exogenic processes, such as rainfall and erosion, accompanied by numer-

Table 1. Data from Global CMT catalog.

Date	Lat	Long	M_w	Strike	Dip	Slip
29.4.1991	42.6	43.61	6.9	288/87	39/53	106/77
29.4.1991	42.38	43.75	6.1	261/62	41/50	104/78
3.5.1991	42.54	42.94	5.6	315/87	47/55	127/57
15.6.1991	42.58	43.07	6.2	138/16	49/58	44/130

ous landslides of different scales (Gracheva and Golyeva, 2010; Jibson et al., 1991; Nikolaeva et al., 2014).

2.1 The Racha earthquake 1991

One of the largest recorded earthquakes ($M_s = 7.0$) occurred at 09:12 GMT (+5 h LT) on 29 April 1991 in the Greater Caucasus, Georgia, Racha region (Fuenzalida et al., 1997). There was no observed tectonic surface rupture associated with this earthquake; however dozens of fatalities occurred due to the landslides triggered by this event (Jibson et al., 1991). A series of aftershocks followed the main shock, spanning several months. There were several significant aftershocks with a few tens of kilometers from the main shock (see Table 1). Several authors indicated four aftershock clusters (Triep et al., 1995; Fuenzalida et al., 1997).

The focal mechanism solution was obtained from the Harvard centroid moment tensor and corresponding to a pure thrust fault dipping to the north (strike = 288°, dip = 39°, rake = 106°). Later, the source parameters were extracted from teleseismic body-wave inversion for the meaningful aftershocks and showed thrust mechanisms on roughly E–W-oriented planes for the main shock. However, the cluster in the east shows a trust fault N–S-oriented (Fuenzalida et al., 1997).

2.2 The Racha earthquake 2009

On 7 September 2009 at 22:41 GMT (+5 h LT), an earthquake with a moment magnitude $M_w = 6.0$ occurred in northern Georgia at a depth of 13.4 km (Fig. 1). The main shock epicenter was located ~80 km north-east of the city of Kutaisi in the Oni district of the Racha–Lechkhumi region. The main shock was felt in Tbilisi (155 km south-east of the event), the capital of Georgia, and in the west of Georgia (Gori and Zugdidi towns). There were no reports of human losses. However, the tremors damaged at least 200 buildings, with some roads blocked by rockfalls and subsequent damage to service lines (information from the Seismic Monitoring Center in Tbilisi, www.seismo.ge).

Within minutes, four aftershocks occurred with magnitudes greater than 4. More aftershocks followed later, with some reaching magnitudes greater than 4 until 13 September 2009. The distribution of aftershocks has same orientation as one of the clusters of the 1991 Racha earthquake (Fig. 1).

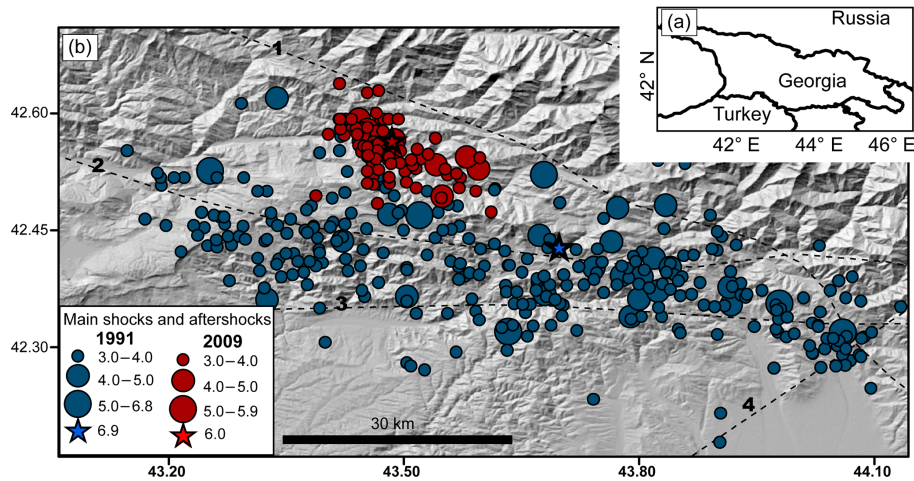


Figure 1. (a) Location of Georgia. (b) Distribution of locations of the Racha main shocks (stars) and aftershocks from 1991 (dark blue dots) and 2009 (dark red dots) with magnitudes greater than 4 (source: the catalog of the Seismic Monitoring Center (SMC) in Georgia, www.seismo.ge). Major faults are shown by black dashed lines (Gamkrelidze and Shengelia, 2007). Numbers on the dashed lines link to the name of the faults. 1. Frontal over thrust of the Caucasus (kinematics: nappes fault), 2. Gagra–Java (kinematics: right-reverse slip fault), 3. Kutaisi–Sachkhere (kinematics: reverse slip fault), and 4. Tskhinvali–Kazbegi (kinematics: left-reverse slip fault). The main city of this area is Oni (lat 42.58, long 43.46) and located close to the main shock 2009 (red star, lat 42.56, long 43.48).

Focal mechanism solutions were obtained from the arrival of *P* waves with only minor variations in the available solutions (Fuenzalida et al., 1997; Vakarchuk et al., 2013). We gathered all available data to form a characterization of the earthquake mechanism. The type of motion was consistently defined as being thrust, roughly dipping to the north-east (Triep et al., 1995). Parameters from the Centroid Moment Tensor (CMT) solution are strike = 314°, dip = 28° and slip = 106°, with the moment tensor solution showing a pure thrust mechanism without a strike-slip component. Also, the focal mechanism solutions and the tectonic structure for the earthquake are available from the EMME (Earthquake Model of the Middle East Region, www.emme-gem.org), CMT (www.globalcmt.org) and Geophysical Survey, Russian Academy of Sciences (www.ceme.gsras.ru) websites.

3 Data and methods

We combined radar images of the Racha region acquired at different times to obtain the two-pass interferometric phase. The interferometric phase contains information about the difference between two independent time measurements of the radar to ground range (Hanssen, 2001). In fact, there are very few SAR acquisitions for this area of central Georgia and for the studied time period (2008–2010) available in the European Space Agency archive, not allowing a detailed deformation study. There are no suitable ERS data available. Envisat (ASAR_IM) data are available for the dates 6 September and 16 November 2009 (same track 178). However, these scenes only partly cover the area investigated. Envisat (ASAR_WS) data are available from different tracks. Also, a coherence of

these scenes is low due to the sensitivity of the C-band to the vegetation. Therefore we concentrate on the Japanese mission ALOS PALSAR, and here use all available data. Only the ascending track (eastward-viewing) of the ALOS satellite, the PALSAR L-band, is available for this area. Therefore one line-of-sight (LOS) component of the deformation field is observable.

We created eight interferograms by using SAR images. Four of the interferograms covered the pre-seismic period, three interferograms covered the co-seismic period, and only one covered the post-seismic period. We formed single-look interferograms using the DORIS processing package (Kampes and Usai, 1999). The phase component associated with the topography was removed from the interferograms, considering the Shuttle Radar Topography Mission Digital Elevation Model (SRTM DEM) at 90 m resolution.

To improve the quality of these interferograms, we applied a multilooking filtering approach so that each pixel of an interferogram represents ~ 200 by ~ 200 m² on the ground. The adaptive filter was used to smooth the speckles in the interferograms (Principe et al., 1993). We then used a two-dimensional phase unwrapping algorithm SNAPHU (Chen and Zebker, 2001; Chen and Zebker, 2002) to obtain unambiguous phase data. To remove the orbital contribution in the phase, we applied a wavelet multi-resolution analysis and robust regression (Shirzaei and Walter, 2011). Atmospheric delay was extracted using the phase-elevation ratio (Zebker et al., 1997). In doing so, we considered the phase-elevation correlation in the south of the image far enough from the earthquake zone. After these corrections and filtering procedures were applied, we observed some relevant signals that

reflect a deformation field. Further evaluation of this deformation field was made in comparison with the dislocation model described below.

Modeling

We used a dislocation model in elastic half space (Okada, 1985) to extract the possible deformation pattern due to the 2009 Racha earthquake. The model calculates the displacement arising from a defined fault plane position and geometry. The model considers the geometry of the fault plane (length and width), the position of the fault in space (strike, depth, dip, coordinates of upper middle edge of fault) and the displacement components (strike-slip and dip-slip).

We utilized the strike and dip from the above presented average focal mechanism solution. Other parameters were calculated based on the known moment magnitude and epicenter of the earthquake. For the first approximation, we assumed that the fault size was 10 by 10 km (Donald et al., 1994). Assuming the moment magnitude (M_w) of 6.0, we can estimate an average displacement (D) of 0.33 m, with a rigidity constant (3×10^{11} dyne cm^{-2}) and the seismic moment from the formula of Hanks and Kanamori (1979).

4 Results

4.1 InSAR

All pre-seismic interferograms lack significant deformation in the Racha region (Fig. 2a–d). This inactivity is confirmed by three different interferograms. Three co-seismic interferograms, in turn, show a deformation signal around the fault zone area with consistent scale (Fig. 2e–g). The deformation field is elongated NW–SE and occurs in the region of the aftershocks following the 2009 event. The long axis is about 15 km, parallel to the seismogenic fault constrained earlier (Gamkrelidze and Shengelia, 2007). The maximum value of deformation reached is 10 cm in the LOS. The deformation is interpreted to be mostly due to uplift in the region north of the alleged fault (Fig. 1). The interferogram 20090904–20091020 (yyyymmdd) is built from acquisitions 4 days before the earthquake and 42 days after (Fig. 2f). This interferogram has a good quality (coherence is higher than 0.7), and it includes the phase changes associated with main event and significant aftershocks (Table 1). The other small aftershocks ($M < 4.5$) did not contribute to the deformation signal based on InSAR analysis (Dawson and Tregoning, 2007). The observed deformation by InSAR has a good correlation with the distribution of aftershocks. We note that the three co-seismic interferograms all use the same slave image. Building independent interferograms was not feasible because of limited high-quality data in the archive for the central Georgia.

One post-seismic interferogram has a slightly poor quality (coherence is low than 0.4) (Fig. 2h). However, it shows no clear deformation signal.

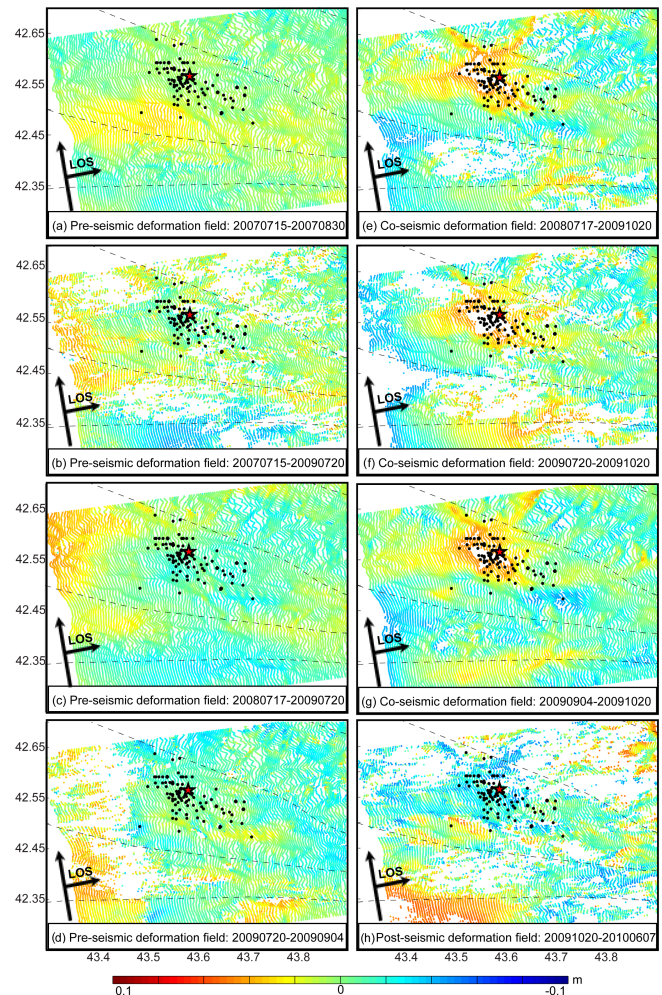


Figure 2. (a–d) Pre-seismic, (e–g) co-seismic and (h) post-seismic deformation fields. The star is the location of the main shock 2009. The black dots are the epicenters of the aftershocks from 2009 with magnitudes greater than 4 (from the catalog of the Seismic Monitoring Center (SMC) in Georgia, www.seismo.ge). Major faults are shown by black dashed lines (Gamkrelidze and Shengelia, 2007). Red colors represent movement toward the ascending satellite.

4.2 Okada model

Our initial dislocation elastic half-space model is based on the main event focal mechanism, CMT solution for the Racha earthquake 2009: strike = 314° and dip = 28° (Fig. 3a). The dip slip of 0.33 m is based on the assumption that the fault is a rectangle and has the parameters length = 10 km and width = 10 km. The depth (10 km) and position is in the middle of the fault plane and was calculated based on knowledge of the earthquake's epicenter. The model generally reproduces the distribution of deformation, as shown by the residuals when subtracted from the InSAR data (Fig. 3a).

The shallowest edge of the fault, however, is not identical to the main orientation of the deformation from the In-

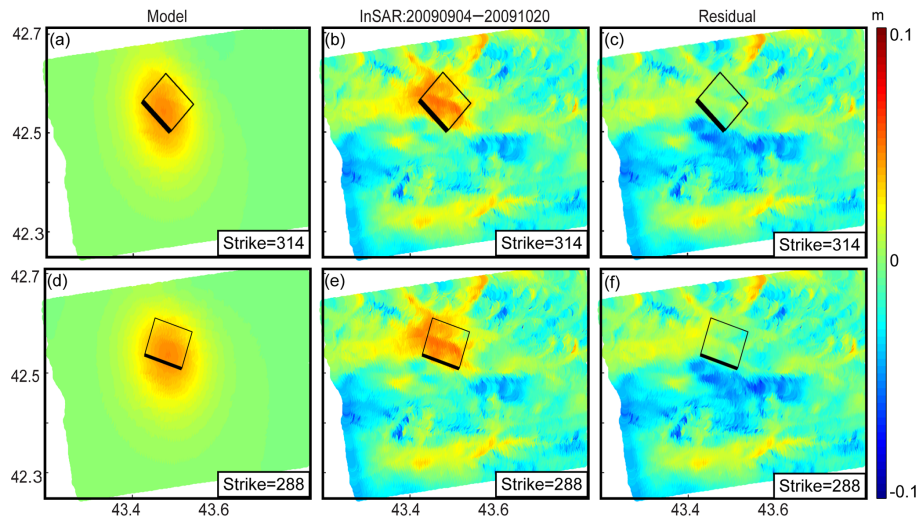


Figure 3. Preliminary results of our forward modeling. (a) Model based on the CMT solution, (b) InSAR interferogram and (c) residual (right) between the observations (b) and model (a). (d) Same model as in the previous case, but with a different strike value, (e) InSAR interferogram and (f) residual between the observations (e) and model (d). The black frames show the projection of fault plane.

SAR observations in modeling case (Fig. 3a). We found that the modeled deformation of a fault oriented 288° from north clockwise better fits the deformation observed in the InSAR results. This trend is also in agreement with the 1991 Racha earthquake, as will be further discussed below. To understand the mechanism of the fault, we had to consider the rupture geometry within the context of previous earthquakes.

5 Discussion

Using satellite radar interferometry, we investigated the displacement associated with the 2009 Racha earthquake. We assessed the ALOS radar data catalog and processed data that covered the earthquake area and the times around the event. The distribution of deformation and aftershocks of the 2009 earthquake have a good correlation with one of the aftershock clusters of the 1991 earthquakes. How might these two events be related?

A comparison of the epicenters from the 1991 and 2009 events reveals the same latitude and a difference of only 0.1° in longitude (the local catalog data). Also, as we described before, the deformation InSAR trench is well fit by a model with a strike = 288° (Fig. 3b). This strike presents the Harvard CMT solution for the 1991 Racha earthquake (Fuenzalida et al., 1997). Therefore, the interesting question is whether the 2009 earthquake occurred on exactly the same fault as the 1991 earthquake and, if so, did the 2009 earthquake fill a seismogenic gap? Answering this question is challenging because of the complexity in the rupture geometries and dynamics of these events (Fuenzalida et al., 1997; Vakarchuk et al., 2013).

The fault system for the 1991 Racha earthquake was formed by four subsources using body wave inversion (Fuenzalida et al., 1997). One subsource significantly dominates the others. Therefore, the model presents a simple single rupture pattern. Based on observations of separate clusters of aftershocks (Arefiev et al., 2006), a model with three complex subsources was created (Vakarchuk et al., 2013). Two subsources represent a thrust type of motion. The reverse type of motion was hypothesized for one of the other subsources. Due to this complexity, it is possible that the use of a simple model does not fit well with the true fault.

The best-fit model determined by InSAR suggests the strike is 288° instead of 314° (CMT), which could be explained by control of local structures. Also, based on the Harvard CMT solution, the dip of the fault might be steeper close to the surface, which was also confirmed by InSAR observation. Vakarchuk et al. (2013) propose a hypocentral depth of the 2009 earthquake of 7 instead of 15 km, according to the CMT catalog (Vakarchuk et al., 2013). Although a surface rupture was not observed (Arefiev et al., 2006), a large number of landslides occurred during and after the Racha 1991 earthquake (Jibson et al., 1991). The distribution of the strongest co-seismic deformations in the Racha earthquake 1991 area (Arefiev et al., 2006; Jibson et al., 1994) is similar to the observed InSAR co-seismic deformations associated with the Racha 2009 earthquake. In addition, the 2009 Racha earthquake triggered landslide activity (Nikolaeva et al., 2014). Consequently, the observed co-seismic deformation likely presents the cumulative effects of the landslides.

The comparison of possible faults for the earthquakes from the 1991 and 2009 (Fig. 4) might imply that the earthquakes are migrating to the north-west. The fault rupture of the

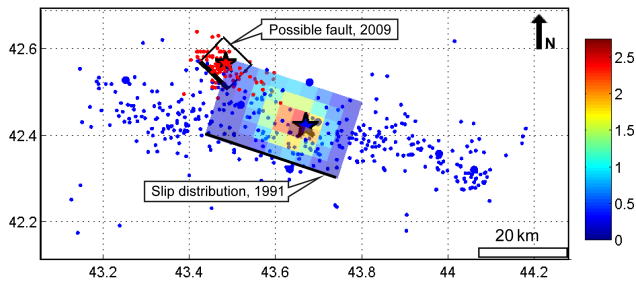


Figure 4. Surface projection of the co-seismic slip distribution of Tan and Taymaz (2006) for the 1991 earthquake. The blue dots are the aftershocks ($M > 3$) and main shock (blue star) of the earthquake to the $M_w = 6.9$ from Seismic Monitoring Center (SMC) in the Georgia catalog. The red dots represent the aftershocks located by SMC from the time of the earthquake to the $M_w = 6$ (red star) event of 7 September 2009. The black frame presents the possible fault plane for the 2009 earthquake, calculated with Okada code based on the CMT solution. Bold lines show the edge of planes close to the surface.

earthquake 2009 may belong to the same fault system that was active in 1991.

Limitations of the herein discussed results mainly may come from the quality and quantity of the InSAR data. Only one viewing component was available, and a small amount of radar data has been archived by the space agency. Therefore all co-seismic interferograms use the same slave image. Possibly this one image contributes noise and/or artifact components, which is then present in all generated interferograms. However, the same slave image is used in post-seismic interferograms, which do not show this deformation pattern. Despite this, the presented InSAR results allow us to develop a general concept about the displacement occurrence and are the only geodetic source available for the studied event.

6 Conclusions

The central region of Georgia repeatedly suffers from earthquakes and landslides. Here, we investigated the recent 2009 Racha earthquake by applying the InSAR method and modeling. We used the multi-temporal ALOS satellite L-band radar images, acquired in ascending mode for the period before, during and after the earthquake. We generated two-pass interferograms and after filtering could identify a significant signal that likely reflects the co-seismic displacement field. The observed InSAR ground deformation is around 10 cm in LOS and probably comes from the cumulative effects of the main shock, aftershocks and triggering events. The deformation model of the 2009 Racha earthquake is in a good agreement with the observed InSAR deformation signal. Results suggest that the 2009 Racha earthquake ($M_w = 6.0$) occurred on the same or sub-parallel fault as the 1991 event. A high spatial resolution of the InSAR data allows the tracking

of a distribution of deformation due to the earthquake in the high mountain Racha region, which is difficult to access.

Our research demonstrates the ability of the InSAR L-band to observe deformations arising from small tectonic events and provides new insights into the tectonic processes of the Caucasus based on radar remote-sensing data. Nowadays with the availability of modern satellites and background missions (e.g., Sentinel), the availability of data for future earthquakes will certainly be improved. Further, InSAR data have the potential to allow us to learn more about the rupture process of earthquakes in the years after the initial event, also including rock avalanches and landslides. Thus, the mapping of the deformation zone after an earthquake reveals the distribution density of landslides in the Racha area.

7 Data availability

The remote sensing data used in this research are freely available via the European Space Agency (ESA) Earth Observation website (<https://earth.esa.int>).

The Supplement related to this article is available online at doi:10.5194/nhess-16-2137-2016-supplement.

Acknowledgements. The authors are grateful to Onur Tan for providing a slip distribution of the 1991 Racha earthquake and discussion. Also we would like to acknowledge Alessandro Parizzi and Hannes Bathke for examination of our interferograms.

The article processing charges for this open-access publication were covered by a Research Centre of the Helmholtz Association.

Edited by: R. Lasaponara

Reviewed by: two anonymous referees

References

- Adamia, S., Alania, V., Chabukiani, A., Chichua, G., Enukidze, O., and Sadradze, N.: Evolution of the Late Cenozoic Basins of Georgia (SW Caucasus): A Review, Geological Society, London, Special Publications, 340, 239–259, doi:10.1144/SP340.11, 2010.
- Arefiev, S. S., Rogozhin, E. A., Bykova, V. V., and Dorbath, C.: Deep Structure of the Racha Earthquake Source Zone from Seismic Tomography Data, *Izvestiya, Physics of the Solid Earth*, 42, 27–40, doi:10.1134/S1069351306010034, 2006.
- Balassanian, S., Ashirov, T., Chelidze, T., Gassanov, A., Kondorskaya, N., and Molchan, G.: Seismic Hazard Assessment for the Caucasus Test Area, *Ann. Geofis.*, 42, 1139–1151, 1999.
- Bell, J. W., Amelung, F., and Henry, C. D.: InSAR Analysis of the 2008 Reno-Mogul Earthquake Swarm: Evidence for Westward

- Migration of Walker Lane Style Dextral Faulting, *Geophys. Res. Lett.*, 39, L18306, doi:10.1029/2012GL052795, 2012.
- Burgmann, R., Schmidt, D., Nadeau, R. M., d'Alessio, M., Fielding, E., Manaker, D., McEvilly, T. V., and Murray, M. H.: Earthquake Potential Along the Northern Hayward Fault, California, *Science*, 289, 1178–1183, 2000.
- Chen, C. W. and Zebker, H. A.: Two-Dimensional Phase Unwrapping with Use of Statistical Models for Cost Functions in Non-linear Optimization, *J. Opt. Soc. Am.*, 18, 338–351, 2001.
- Chen, C. W. and Zebker, H. A.: Phase Unwrapping for Large SAR Interferograms: Statistical Segmentation and Generalized Network Models, *IEEE T. Geosci. Remote Sens.*, 40, 1709–1719, 2002.
- Dawson, J. and Tregoning, P.: Uncertainty Analysis of Earthquake Source Parameters Determined from InSAR?: A Simulation Study, *J. Geophys. Res.*, 112, 1–13, doi:10.1029/2007JB005209, 2007.
- Donald, L., Coppersmith, W. J., and Coppersmith, K. J.: New Empirical Relationships among Magnitude, Rupture Length, Rupture Width, Rupture Area, and Surface Displacement, *B. Seismol. Soc. Am.*, 84, 974–1002, 1994.
- Fuenzalida, H., Rivera, L., Haessler, H., Legrand, D., Philip, H., Dorbath, L., McCormack, D., Arefiev, S., Langer, C., and Cisternas, A.: Seismic Source Study of the Racha-Dzhava (Georgia) Earthquake from Aftershocks and Broad-Band Teleseismic Body-Wave Records: An Example of Active Nappe Tectonics, *Geophys. J. Int.*, 130, 29–46, doi:10.1111/j.1365-246X.1997.tb00985.x, 1997.
- Funning, G. J.: Surface Displacements and Source Parameters of the 2003 Bam (Iran) Earthquake from Envisat Advanced Synthetic Aperture Radar Imagery, *J. Geophys. Res.*, 110, B09406, doi:10.1029/2004JB003338, 2005.
- Gamkrelidze, I. P. and Shengelia, D. M.: Pre-Alpine Geodynamics of the Caucasus, Suprasubduction Regional Metamorphism and Granitoid Magmatism, *Bull. of Georgian National Acad. of Science*, 175, 57–65, 2007.
- Gracheva, R. and Golyeva, A.: Landslides in Mountain Regions: Hazards, Resources and Information, in: *Geophysical Hazards, International Year of Planet Earth*, edited by: Beer, T., 249–260, Dordrecht, Springer Netherlands, available at: <http://www.springerlink.com/index/10.1007/978-90-481-3236-2>, 2010.
- Hanks, T. C. and Kanamori, H.: A Moment Magnitude Scale, *J. Geophys. Res.*, 84, 2348, doi:10.1029/JB084iB05p02348, 1979.
- Hanssen, R. F.: *Radar Interferometry: Data Interpretation and Error Analysis*, Kluwer Academic Publishers, Dordrecht, 2001.
- Jibson, R. W., Randall, W., and Prentice, C. S.: Ground Failure Produced by the 29 April 1991 Racha Earthquake in Soviet Georgia, *U.S. Geological Survey*, 10, http://books.google.de/books/about/Ground_Failure_Produced_by_the_29_April.html?id=xNYsYgEACAAJ&redir_esc=y, 1991.
- Jibson, R. W., Prentice, C. S., Borissoff, B. A., Rogozhin, E. A., and Langer, C. J.: Some Observations of Landslides Triggered by the 29 April 1991 Racha Earthquake, Republic of Georgia, *Bulletin Seismological Society of America*, 84, 963–973, <http://www.scopus.com/inward/record.url?eid=2-s2.0-0028667427&partnerID=40&md5=ab8f839699fc3eacbd45a3f1854a8530>, 1994.
- Kampes, B. and Usai, S.: Doris: The Delft Object-Oriented Radar Interferometric Software, In *2nd International Symposium on Operationalization of Remote Sensing Enschede The Netherlands*, available at: <http://doris.tudelft.nl/Literature/kampes99.pdf>, 1999.
- Lilienberg, D. A.: *Obschie i regionalniye zakonomernosti sovremennoi geodinamiki Kavkaza (po geomorfologicheskim i instrumentalnim dannim): Sovremenniy Dvizheniya Zemnoi Kori*, Naukova Dumka, Kiev, 204–217, 1980 (in Russian).
- Lin, J. and Stein, R. S.: Stress Triggering in Thrust and Subduction Earthquakes and Stress Interaction between the Southern San Andreas and Nearby Thrust and Strike-Slip Faults, *J. Geophys. Res.*, 109, 1–19, doi:10.1029/2003JB002607, 2004.
- Massonnet, D., Rossi, M., Carmona, C., Adragna, F., Peltzer, G., Feigl, K., and Rabaut, T.: The Displacement Field of the Landers Earthquake Mapped by Radar Interferometry, *Nature*, 364, 138–142, doi:10.1038/364138a0, 1993.
- Nikolaeva, E., Walter, T. R., Shirzaei, M., and Zschau, J.: Landslide observation and volume estimation in central Georgia based on L-band InSAR, *Nat. Hazards Earth Syst. Sci.*, 14, 675–688, doi:10.5194/nhess-14-675-2014, 2014.
- Okada, Y.: Surface Deformation due to Shear and Tensile Faults in a Half-Space, *Int. J. Rock Mech. Min.*, 75, 1135–1154, doi:10.1016/0148-9062(86)90674-1, 1985.
- Philip, H., Cisternas, A., Gvishiani, A., and Gorshkov, A.: The Caucasus: An Actual Example of the Initial Stages of Continental Collision, *Tectonophysics*, 161, 1–21, doi:10.1016/0040-1951(89)90297-7, 1989.
- Pondard, N., Armijo, R., King, G. C. P., and Meyer, B.: Fault Interactions in the Sea of Marmara Pull-Apart (North Anatolian Fault), *Earthquake Clustering and Propagating Earthquake Sequences*, *Geophys. J. Int.*, 171, 1185–1197, doi:10.1111/j.1365-246X.2007.03580.x, 2007.
- Principe, J. C., De Vries, B., and De Oliveira, P. G.: The Gamma-Filter—a New Class of Adaptive IIR Filters with Restricted Feedback, *IEEE T. Signal Proces.*, 41, 649–656, 1993.
- Reilinger, R. E., Ergintav, S., Bürgmann, R., McClusky, S., Lenk, O., Barka, A., Gurkan, O., Hearn, L., Feigl, K. L., Cakmak, R., Aktug, B., Ozener, H., and Töksoz, M. N.: Coseismic and Postseismic Fault Slip for the 17 August 1999, $M = 7.5$, Izmit, Turkey, *Earthquake Science*, 289, 1519–1524, 2000.
- Reilinger, R., McClusky, S., Vernant, P., Lawrence, S., Ergintav, S., Cakmak, R., Ozener, H., Kadirov, F., Guliev, I., Stepanyan, R., Nadariya, M., Hahubia, G., Mahmoud, S., Sakr, K., ArRajehi, A., Paradissis, D., Al-Aydrus, A., Prilepin, M., Guseva, T., Evren, E., Dmitrotsa, A., Filikov, S. V., Gomez, F., Al-Ghazzi, R., and Karam, G.: GPS Constraints on Continental Deformation in the Africa-Arabia-Eurasia Continental Collision Zone and Implications for the Dynamics of Plate Interactions, *J. Geophys. Res.*, 111, 1–26, doi:10.1029/2005JB004051, 2006.
- Shirzaei, M. and Walter, T. R.: Estimating the Effect of Satellite Orbital Error Using Wavelet-Based Robust Regression Applied to InSAR Deformation Data, *IEEE T. Geosci. Remote Sens.*, 49, 4600–4605, available at: http://ieeexplore.ieee.org/xpls/abs_all.jsp?arnumber=5779729, 2011.
- Stein, R. S., Barka, A. A., and Dieterich, J. H.: Earthquake Stress Triggering, *Geophys. J. Int.*, 128, 594–604, 1997.
- Tan, O. and Taymaz, T.: Active Tectonics of the Caucasus: Earthquake Source Mechanisms and Rupture Histories Ob-

- tained from Inversion of Teleseismic Body Waveforms, Geological Society of America Special Papers, 409, 531–578, doi:10.1130/2006.2409(25), 2006.
- Triep, E. G., Abers, G. A., Lerner-Lam, A. L., Mishatkin, V., Zakharchenko, N., and Starovoit, O.: Active Thrust Front of the Greater Caucasus: The April 29, 1991, Racha Earthquake Sequence and Its Tectonic Implications, *J. Geophys. Res.*, 100, 4011–4033, available at: <http://www.agu.org/pubs/crossref/1995/94JB02597.shtml>, 1995.
- Vakarchuk, R. N., Tatevossian, R. E., Aptekman, Zh. Ya., and Bykova, V. V.: The 1991 Racha Earthquake, Caucasus: Multiple Source Model with Compensative Type of Motion, *Izvestiya, Physics of the Solid Earth*, 49, 653–669, doi:10.1134/S1069351313050121, 2013.
- van Westen, C. J., Straatsma, M. W., Turdukulov, U. D., Feringa, W. F., Sijmons, K., Bakhtadze, K., Janelidze, T., Kheladze, N., Natsvlshvili, L., Tkhelidze, N., Gaprindashvili, G., Megrelidze, I., Geladze, G., Gloveli, V., Sukhishvili, L., Elashvili, M., Tsamalashvili, T., and Feliciano, I. T.: Atlas of Natural Hazards and Risk in Georgia, edited by: van Westen, C. J., CENN Caucasus Environmental NGO Network, 2012.
- Wang, R., Xia, Y., Grosser, H., Wetzel, H.-U., Kaufmann, H., and Zschau, J.: The 2003 Bam (SE Iran) Earthquake: Precise Source Parameters from Satellite Radar Interferometry, *Geophys. J. Int.*, 159, 917–922, doi:10.1111/j.1365-246X.2004.02476.x, 2004.
- Zebker, H. A., Rosen, P. A., and Hensley, S.: Atmospheric Effects in Interferometric Synthetic Aperture Radar Surface Deformation and Topographic Maps, *Geophysical Res.*, 102, 7547–7563, available at: <http://192.102.233.13/journals/jb/v102/iB04/96JB03804/96JB03804.pdf>, 1997.